

Poly (3-hydroxybutyrate-co-3-hydroxyvalerate)/fibrinogen/bredigite nanofibrous membranes and their integration with osteoblasts for guided bone regeneration

Monireh Kouhi ^{1,2}, Venugopal Jayarama Reddy,^{2,3} Mohammadhossein Fathi,¹ Morteza Shamanian,¹ Afsaneh Valipouri,⁴ Seeram Ramakrishna²

¹Biomaterials Research Group, Department of Materials Engineering, Isfahan University of Technology, Isfahan, Iran

²Center for Nanofibers and Nanotechnology, Department of Mechanical Engineering, National University of Singapore, Singapore

³Faculty of Industrial Sciences & Technology, Universiti Malaysia Pahang, Kuantan, Malaysia

⁴Department of Textile Engineering, Isfahan University of Technology, Isfahan, Iran

Received 26 August 2018; revised 30 November 2018; accepted 9 January 2019

Published online 28 January 2019 in Wiley Online Library (wileyonlinelibrary.com). DOI: 10.1002/jbm.a.36607

Abstract: Guided bone regeneration (GBR) has been established to be an effective method for the repair of defective tissues, which is based on isolating bone defects with a barrier membrane for faster tissue reconstruction. The aim of the present study is to develop poly (hydroxybutyrate-co-3-hydroxyvalerate) (PHBV)/fibrinogen (FG)/bredigite (BR) membranes with applicability in GBR. BR nanoparticles were synthesized through a sol-gel method and characterized using transmission electron microscopy and X-ray diffractometer. PHBV, PHBV/FG, and PHBV/FG/BR membranes were fabricated using electrospinning and characterized by scanning electron microscopy, Fourier transform infrared spectroscopy, contact angle, pore size, thermogravimetric analysis and tensile strength. The electrospun PHBV, PHBV/FG, and PHBV/FG/BR nanofibers were successfully obtained with the mean diameter ranging 240–410 nm. The results showed that Young's modulus and ultimate strength of the PHBV membrane reduced upon blending with FG and increased by further incorporation of BR nanoparticles. Moreover hydrophilicity of

the PHBV membrane improved on addition of FG and BR. The in vitro degradation assay demonstrated that incorporation of FG and BR into PHBV matrix increased its hydrolytic degradation. Cell-membrane interactions were studied by culturing human fetal osteoblast cells on the fabricated membrane. According to the obtained results, osteoblasts seeded on PHBV/FG/BR displayed higher cell adhesion and proliferation compared to PHBV and PHBV/FG membrane. Furthermore, alkaline phosphatase activity and alizarin red-s staining indicated enhanced osteogenic differentiation and mineralization of cells on PHBV/FG/BR membranes. The results demonstrated that developed electrospun PHBV/FG/BR nanofibrous mats have desired potential as a barrier membrane for guided bone tissue engineering. © 2019 Wiley Periodicals, Inc. *J Biomed Mater Res Part A*: 107A: 1154–1165, 2019.

Key Words: bredigite, fibrinogen, guided bone tissue engineering, nanofibrous membranes, poly (3-hydroxybutyrate-co-3-hydroxyvalerate)

How to cite this article: Kouhi M, Jayarama Reddy V, Fathi M, Shamanian M, Valipouri A, Ramakrishna S. 2019. Poly (3-hydroxybutyrate-co-3-hydroxyvalerate)/fibrinogen/bredigite nanofibrous membranes and their integration with osteoblasts for guided bone regeneration. *J Biomed Mater Res Part A* 2019;107A:1154–1165.

INTRODUCTION

Guided bone regeneration (GBR) demonstrated to be an effective method to regenerate bone tissue in the defect sites, which involve the creation and maintenance of a secluded space by using a barrier membrane to prevent the migration of epithelial and other soft tissues into the osseous defective area, thereby allowing sufficient time for the regeneration of bone.^{1–3} To achieve the effective GBR approach, the barrier membrane should have specific properties such as biocompatibility, bioactivity (osteoconductivity), cell-occlusiveness, mechanical stability (space maintaining ability), resorbability, and clinical operability.^{4,5} A number of natural and synthetic polymers have been developed as the

resorbable membranes for GBR applications such as poly (lactic-co-glycolic acid), polycaprolactone, poly hydroxyalkanoates, gelatin, chitosan, and collagen.^{2,4–7} Among all kinds of membrane polymers, poly (3-hydroxybutyrate-co-3-hydroxyvalerate) (PHBV) is a promising biomaterial which has been extensively investigated for bone tissue engineering. PHBV is a biodegradable polyester, produced by bacteria with attractive characteristics in the field of biomedical applications, such as natural origin, biocompatibility, and biodegradability.^{8,9} Moreover, PHBV degrades in vivo into hydroxybutyric acid, which is a normal constituent of human blood.¹⁰ However, when considering its application in bone tissue engineering, PHBV is associated with several major

Correspondence to: M. Kouhi; e-mail: monireh.kouhi@gmail.com

disadvantages such as hydrophobic nature and lack of cell-recognizable sites, low degradation rate compared with typical bone healing time and poor bioactivity (bone regeneration capacity).¹¹ Combination of PHBV with inorganic bioactive phases and natural components with higher hydrophilicity, bioactivity and degradation rate may be an effective approach to overcome its intrinsic shortcoming. Bredigite (BR, $\text{Ca}_7\text{MgSi}_4\text{O}_{16}$) is a magnesium silicate based bioceramic, which have the ability to form bone-like apatite in the simulated body fluid and can enhance cellular activity.¹² Wu et al.¹³ demonstrated the enhanced mechanical properties and higher apatite mineralization ability and degradation rate of BR bioceramic compared to Ca-P ones as well as the ability to support the osteoblasts adhesion and proliferation. The application of BR bioceramic in bone tissue engineering was reported by Zhou et al.,¹⁴ whereby the ionic products from the dissolution of the BR significantly enhanced the periodontal ligament cells proliferation, alkaline phosphatase (ALP) activity, mineralization, and osteogenesis/cementogenesis-related gene/protein expression in bone tissue regeneration.

Fibrinogen, a fibrous blood plasma glycoprotein, has long been of interest in creating scaffolds for wound healing and hemostasis. Its inherent ability to induce cell adhesion, proliferation and migration, as well as its degradability, non-immunogenicity and ability to undergo biomimetic mineralization, make it an attractive biopolymer for the development of bone tissue engineering scaffolds.^{15,16} Considering the advantages of BR and fibrinogen toward cellular activity, we applied these two components to overcome the shortcoming of PHBV polymer in GBR applications.

Nanofibrous materials have been widely used as desired membranes for tissue engineering applications. In addition to inherent flexibility, nanofibrous membranes can provide high area-to-volume ratios structures which mimic the extracellular matrix (ECM) of native tissue, hence capable of inducing cellular adhesion and growth.¹⁷⁻¹⁹ The most studied techniques for fabricating nanofibrous membrane are phase separation, self-assembly, and electrospinning.²⁰ Among them, electrospinning attracted rapidly growing interests due to its ease of use and affordable instrumental set-up without any complex equipment.²¹ Moreover, mechanical, chemical and biological characteristics of electrospun structures can be altered in order to obtain favorable biomimetic materials with enhanced cellular responses.¹⁶ Furthermore, since the pore size of the electrospun membranes is smaller than the average cell size, the membranes can prevent cell penetration but allow nutrient materials and oxygen diffusion into, and metabolic waste out of the area of tissue regeneration.²²

In the present study, a novel biomimetic GBR membrane was fabricated using PHBV, BR nanoparticles and fibrinogen via electrospinning. We expected that the combination of BR nanoparticles and fibrinogen with PHBV in the form of nanofibrous structures would produce a biomimetic membrane with enhanced mechanical strength, bioactivity, and cellular response. The morphological, chemical, and mechanical properties of the resultant membranes were investigated,

and the cell-membranes interactions were evaluated by culturing human fetal osteoblast (hFob) cells on the developed membranes to assess the suitability of the developed membranes for guided bone regeneration.

MATERIALS AND METHODS

Preparation of BR nanoparticles

BR nanoparticles were synthesized using sol-gel method as described in our previous study.²³ Briefly, tetraethyl orthosilicate (TEOS, Merck) was mixed with nitric acid (2 M, Merck) and water (mole ratio: TEOS/nitric acid/water = 1:0.08:4) and hydrolyzed for 30 min under stirring. $\text{Ca}(\text{NO}_3)_2 \cdot 4\text{H}_2\text{O}$ and $\text{Mg}(\text{NO}_3)_2 \cdot 6\text{H}_2\text{O}$ were then added to the mixture (mole ratio: TEOS/ $\text{Ca}(\text{NO}_3)_2 \cdot 4\text{H}_2\text{O}$ / $\text{Mg}(\text{NO}_3)_2 \cdot 6\text{H}_2\text{O}$ = 4:7:1), and the solution was stirred at room temperature for 5 h. The prepared sol was kept at 60°C for 24 h and dried at 120°C for 48 h to get a dried gel, which was then calcined at 1150°C for 2 h with a heating rate of 5°C/min. Finally, it was ball-milled in a zirconia mechanical ball mill and characterized using transmission electron microscopy (TEM; JEOL JEM-2010F) and X-ray diffractometer (XRD; Philips X'Pert-MPD, Cu K α radiation at 30 mA and 40 kV, at a scan rate of 3°/min).

Fabrication of nanofibrous membranes

PHBV, PHBV/fibrinogen, and PHBV/fibrinogen/BR nanofibrous membranes were fabricated using electrospinning technique. Briefly, PHBV (TianAn Enmat chemical company, China) was dissolved in 1,1,1,3,3,3 hexafluoro-2-propanol (HFIP, Sigma) to obtain 8 wt % pure PHBV solution. PHBV/fibrinogen solution was prepared by dissolving PHBV polymer and fibrinogen (Sigma; PHBV/fibrinogen: 80/20 [w/w]) in HFIP to make a total concentration of 8 wt %. To prepare PHBV/fibrinogen/BR solution, BR nanoparticles (10 wt % of total content) was sonicated for 30 min in HFIP; further PHBV/fibrinogen (80/20) was added to this mixture to obtain 8 wt % polymer composite solutions. All prepared solution including pure PHBV, PHBV/fibrinogen, and PHBV/fibrinogen/BR solution were stirred overnight at room temperature, loaded into a 3 mL syringe, and pumped through a needle of 0.5 mm internal diameter. The high voltage (Gamma High Voltage Research, FL) of 14 kV was applied to the polymeric solution. The constant flow rate of 1 mL/h was fixed using a syringe pump (KD 100 Scientific Inc., Holliston, MA) at a distance of 15 cm which maintained between the needle tip and the collector. The electrospun nanofibrous membranes were dried in a vacuum oven for 24 h to eliminate residual solvent and then kept in a desiccator for further characterization and cell culture study. PHBV/fibrinogen and PHBV/fibrinogen/BR nanofibrous membrane were termed as PHBV/FG and PHBV/FG/BR, respectively.

Characterization of nanofibrous membranes

The morphology of electrospun membranes was observed by field-emission scanning electron microscopy (FESEM: HITACHI S-4300, Japan). The diameter of the obtained nanofibers was measured from FESEM images using ImageJ

software (Image Java, National Institutes of Health, Bethesda, MD). The wet-up/dry-up method of capillary flow porometer (1200-AEHLX capillary flow porometer, Porous Materials Inc., Ithaca, NY) was used to determine the membranes pore diameter. Samples were punched into 20 mm-diameter round mats and their thickness was measured using a micrometer. The pore size was calculated by the software from Porous Media Inc (Ithaca, NY) as a function of the surface tension of the wetting liquid, the contact angle of the wetting liquid, and differential pressure. Surface wettability of the nanofibrous membranes was investigated by a video contact angle system (VCA optima, AST Products, Billerica, MA). The water contact angle on three different positions was measured and recorded for each sample. The mechanical strength of the fabricated membranes was tested and determined using a tabletop tensile tester (Instron 5943) with a load cell of 50 N. The nanofibrous membranes were cut into rectangular strips (10 × 20 mm) mounted vertically on the gripping unit and tested at a crosshead speed of 10 mm/min. Tensile stress, elongation at break and elastic modulus were calculated from the generated tensile stress-strain curves. At least five samples were tested for each type of the membranes. Fourier transform infrared (FTIR) spectroscopic analysis of nanofibrous membranes was performed on Avatar 380 spectrophotometer (Thermo Nicolet, Waltham, MA) over a range of 400–4000 cm⁻¹ at 4 cm⁻¹. Thermal properties of the electrospun membranes were examined by thermogravimetric (TGA) experiments using STA 503 (Bahr, Germany). All the samples were pre-weighed and subjected to a programmed heating in the temperature range of 30°C–600°C at a rate of 10°C/min.

In vitro biodegradation of the nanofibrous membranes

Electrospun membranes were cut into 10 × 10 mm² pieces, weighted, and placed into the plastic tubes containing 10 mL of phosphate buffer solution (PBS, Sigma-Aldrich) at pH 7.3. The tubes were kept at 37°C for 28 days. PBS was replaced with a new solution every 3 days. At each time interval, the samples were washed with water, dried in a vacuum oven at room temperature, and weighed again. The percentage of weight loss was calculated based on the equation: $[(W_0 - W_T)/W_0] \times 100$, where W_0 is the weight of the sample before test and W_T is the weight of the sample after degradation period of time. An average of six measurements was taken for each sample. The changes in the surface morphology of the nanofibrous membranes during degradation assay were visualized by SEM.

Culture of hFob cells

The hFob cells, obtained from the American Type Culture Collection (ATCC, VA 20108, USA), were cultured in Dulbecco's modified eagles medium/nutrient mixture F-12 (DMEM/F12, Sigma Aldrich, Singapore), supplemented with 10% fetal bovine serum (FBS, GIBCO, Invitrogen Corp) and 1% antibiotic solution (Sigma-Aldrich, A5955) in a 75 cm² cell culture flask, which was then incubated in CO₂ incubator at 37°C and 5% CO₂. After confluency, cells were detached by trypsin/EDTA (GIBCO, Invitrogen Corp) and seeded on

the nanofibrous membranes at the seeding density of 10⁴ cells/well. To study cell-membranes interactions, the nanofibrous membranes which were previously collected on the 15 mm coverslips, were placed in a 24-well plate, sterilized using UV light for 2 h, washed three times with PBS for 15–20 min, and immersed in complete medium (DMEM/F12-10% FBS-1% antibiotics) overnight prior to culturing of osteoblasts.

Cell proliferation. The hFob proliferation on the electrospun membranes was evaluated using the colorimetric MTS assay (CellTiter 96 Aqueous One solution; Promega, Madison). The yellow tetrazolium compound in MTS reacts with the viable cells to generate a purple soluble formazan product, which can be detected using absorbance measurements at 490 nm. The amount of generated formazan dye is directly proportional to the number of cells. After 5, 10, and 15 days of cell culture, the media was discarded from the wells and the cells were rinsed with PBS and incubated with MTS reagent (20%) in serum-free medium in 5% CO₂ incubator at 37°C for 3 h. After the incubation period, the obtained dye was aliquoted into 96-well plates and read using a spectrophotometric plate reader (FLUO star OPTIMA, BMG lab Technologies, Germany). The experiments were done in three replicates and the cells grown on tissue culture plastic (TCP) served as the control.

ALP activity. The expression of ALP by cells is a marker of osteoblastic maturation and differentiation, which can be measured by applying alkaline phosphate yellow liquid substrate system for ELISA (Sigma Life Sciences). After 5, 10, and 15 days of culturing, the medium was aspirated from the wells and cells were rinsed with PBS and incubated with ALP solution (400 μL) for 1 h at room temperature. The ALP activity was stopped by addition of 100 μL of 2 N NaOH solution following which the yellow color product was aliquoted in 96-well plates and read in spectrophotometric plate reader at 405 nm.

Alizarin red-S. Alizarin red-S (ARS) staining was used to evaluate calcium-rich deposits produced by hFob. After 5, 10, and 15 days of cell seeding, the nanofibrous membranes with cells were washed thrice with PBS and fixed in ice-cold ethanol (70%) for 1 h. The fixed samples were then rinsed thrice with distilled water and stained with ARS (Sigma Aldrich, 40 mM) for 1 h in an incubator at 37°C. Microscopic images of the stained cells visualizing the mineralization were taken using an optical microscope. For quantitative detection of mineral deposits, the stained cells were washed two times with deionized water and treated with cetylpyridinium chloride (10%, Sigma Aldrich) for 1 h. The desorbed dye was collected and its absorbance was measured at 540 nm using a spectrophotometer (Thermo Spectronic). The experiment was conducted in three replicates to plot the graph for osteoblasts mineralization.

Cell morphology and energy dispersive X-ray spectroscopy (EDS). FESEM was used to evaluate cell morphology and mineral secretion of hFob seeded on different nanofibrous

membranes. After 5 and 15 days of the cell culture, the media was removed from the wells and the samples were rinsed with PBS and fixed with 3% glutaraldehyde in PBS for 3 h. The membrane with cells were then rinsed with distilled water for 15 min and then dehydrated with a series of ethanol solutions of increasing concentrations (30%, 50%, 75%, 90%, and 100% [v/v]). Finally, the cells were treated with hexamethyldisilazane (Sigma Aldrich) and left to dry overnight at room temperature. The dried samples were observed under FESEM-EDS.

Statistical analysis

All experiments were performed three times and the results were shown as the mean value and standard deviations. One-way analysis of variance (ANOVA) with pairwise post-hoc Tukey was used to evaluate the differences between the different groups or time points. A *p* value of 0.05 was considered statistically significant.

RESULTS

Characterization of the nanoparticles and nanofibrous membranes

X-ray diffraction (XRD) pattern and TEM image of the BR nanoparticles are shown in Figure 1. The obtained experimental XRD pattern was in good agreement with the standard card of BR (JCPDS: 036-0399). TEM micrograph indicated the production of irregular shaped nanoparticles with the average size of 25 nm. The typical FESEM images of as-electrospun PHBV, PHBV/FG, and PHBV/FG/BR nanofibrous membranes along with the histograms of the nanofiber diameters are given in Figure 2. The average fiber diameters of the electrospun membranes are summarized in Table I. The bead-free and relatively uniform PHBV nanofibers were obtained with the fiber diameter of 410 ± 61 nm, without the formation of tiny short nanofibers. Blending fibrinogen with PHBV yielded a decrease in average fiber diameter (240 ± 96 nm) for PHBV/FG nanofibers along with the formation of short and tiny nanofiber elongated from the large fibers. On BR nanoparticles incorporation into the

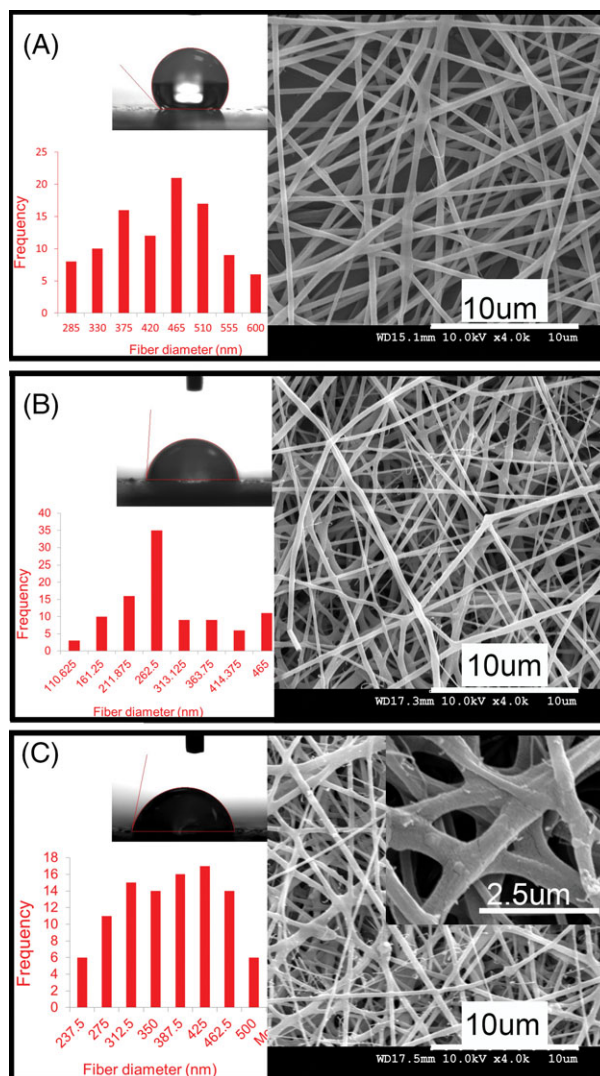


FIGURE 2. FESEM images, corresponding fiber size distribution and images of water droplet on (A) PHBV, (B) PHBV/FG, and (C) PHBV/FG/BR membranes. BR, bredigite; FESEM, field-emission scanning electron microscopy; FG, fibrinogen; PHBV, poly (hydroxybutyrate-co-3-hydroxyvalerate).

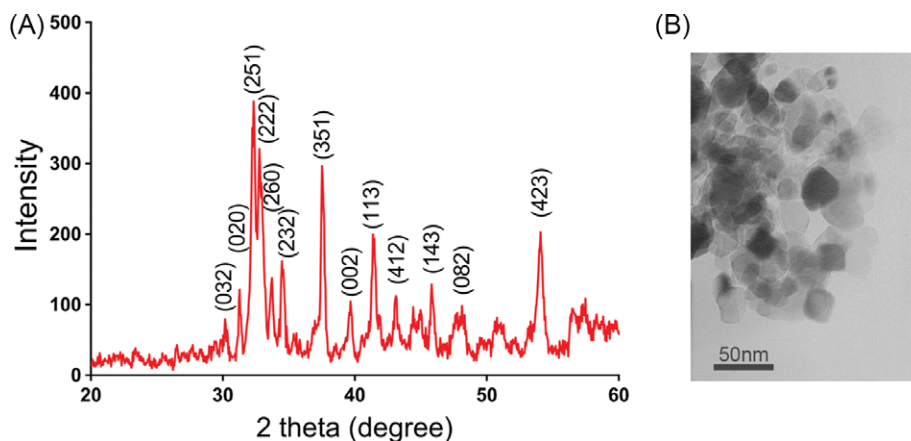


FIGURE 1. Structural properties of bredigite nanoparticles, (a) XRD pattern of bredigite nanoparticles, (b) TEM image of bredigite nanoparticles. TEM, transmission electron microscopy; XRD, X-ray diffraction.

TABLE I. Fiber diameter, contact angle and pore size of PHBV based nanofibrous membranes

Sample	Fiber diameter (nm)	Water contact angle (degree)	Pore size (μm)
PHBV	410 \pm 61	129 \pm 6	2.40 \pm 0.64
PHBV/FG	240 \pm 96	83 \pm 3	1.05 \pm 0.32
PHBV/FG/BR	315 \pm 50	76 \pm 3	1.38 \pm 0.33

Abbreviations: BR, bredigite; FG, fibrinogen; PHBV, poly (hydroxybutyrate-co-3-hydroxyvalerate).

nanofibers, the average fiber diameter increased slightly to 315 \pm 50 nm for PHBV/FG/BR nanofibers compared to PHBV/FG nanofibers.

The surface hydrophilicity of a membrane is a key parameter in inducing cell adhesion and growth, which was studied by measuring the water contact angle throughout this work. The results of water contact angle measurements are summarized in Figure 2 and Table I. PHBV is a naturally hydrophobic polymer showing a water contact angle value of 129° \pm 6°. The incorporation of fibrinogen into the PHBV matrix significantly reduced the water contact angle of PHBV/FG membranes to 83° \pm 3° ($p \leq 0.05$), indicating the improvement in the membranes hydrophilicity. The PHBV/FG/BR membranes exhibited lower contact angle (76° \pm 3°) compared to PHBV/FG membrane as a result of the presence of BR nanoparticles, proving the higher hydrophilicity of PHBV/FG/BR compared to pure PHBV and PHBV/FG membranes. The pore size measurement results presented in Table I indicates that PHBV/FG/BR and PHBV/FG membranes had lower pore diameter (1.38 and 1.05 μm , respectively) when compared to PHBV membranes (2.4 μm). Similarly, PHBV/FG showed the lowest pore size compared to other samples; this might be attributed to the smaller fiber diameter of PHBV/FG.

FTIR spectra of PHBV, PHBV/FG, and PHBV/FG/BR nanofibrous membranes are presented in Figure 3A. The spectra of PHBV membrane displays a peak at 1721 cm^{-1} responsible for C=O stretching band, the peaks ranging 1230–1430 cm^{-1} and 835–955 cm^{-1} corresponds to various aliphatic C–H vibrational bands, and the peaks for C–O

vibrational bands at 1170, 1125, and 1020 cm^{-1} .^{17,24} In the spectra of blended PHBV/FG and PHBV/FG/BR membranes, two peaks at 1640 and 1530 cm^{-1} corresponded to the amide I and amide II bands of fibrinogen, respectively, and a broad peak at about 3350 cm^{-1} , which are characteristic peaks of peptides/protein structures^{16,25} are observed, in addition to typical bands of PHBV. In the spectra of PHBV/FG/BR nanofibers, the peaks at 850 and 961 cm^{-1} attributed to stretching vibration of silicate structure and the peak at 507 cm^{-1} corresponded to Mg–O bands appeared or their intensity increased, in addition to typical bands of PHBV and fibrinogen.^{17,23,26} The obtained results from FTIR analysis confirmed the successful blending of fibrinogen and BR with PHBV nanofibers.

Thermal properties of nanofibrous membranes were evaluated by TGA. Figure 3B shows the TGA diagram of PHBV, PHBV/FG, and PHBV/FG/BR membranes. All nanofibrous membranes showed a single stage thermal decomposition. PHBV decomposed completely in the region of 230°C to 300°C as shown in Figure 3B, while blending fibrinogen with PHBV resulted in prolonged decomposition temperature to 400°C. In the presence of BR nanoparticles, the curves were shifted to the higher temperature indicating an increase in thermal stability of PHBV/FG/BR membranes compared to PHBV and PHBV/FG nanofibers. The residual weight of PHBV/FG/BR membranes at the final test temperature was about 9%, showing the true content of BR nanoparticles in the membrane, proving that the amount of BR nanoparticles added to the PHBV/FG solution before electrospinning was approximately equal to its amount in the PHBV/FG/BR nanofibrous membranes after electrospinning.

Mechanical strength of the prepared nanofibrous membranes was found to be influenced by the composition of the nanofibers. Figure 4A shows the typical stress–strain curves of the PHBV, PHBV/FG, and PHBV/FG/BR nanofibrous membranes. All samples exhibited a linear segment first, followed by a nonlinear curve. Key mechanical parameters including Young's modulus, tensile strength, and elongation at break, obtained from their stress–strain curves, are presented in Figure 4B. The incorporation of fibrinogen into PHBV matrix reduced Young's modulus and tensile strength of PHBV/FG membranes (83.3 \pm 15.5 MPa and 3.68 \pm 1.1 MPa) compared

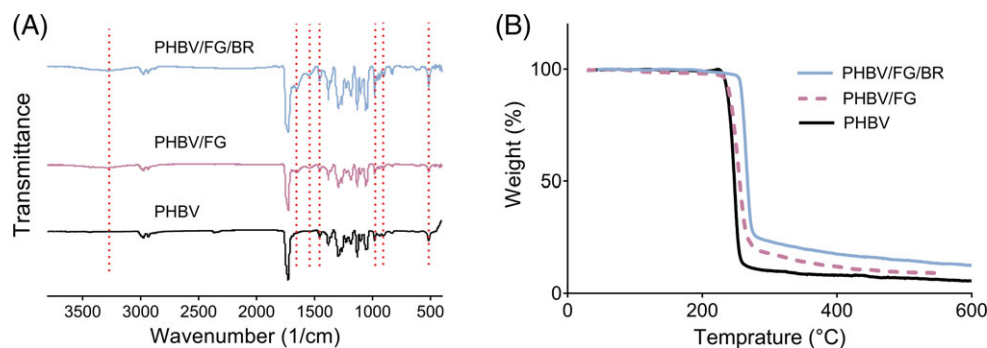


FIGURE 3. Structural properties of membranes (A) FTIR spectra of PHBV, PHBV/FG and PHBV/FG/BR nanofibrous membranes, (B) TGA diagram of PHBV, PHBV/FG and PHBV/FG/BR nanofibrous membranes. BR, bredigite; FG, fibrinogen; FTIR, Fourier transform infrared; PHBV, poly (hydroxybutyrate-co-3-hydroxyvalerate); TGA, thermogravimetric analysis.

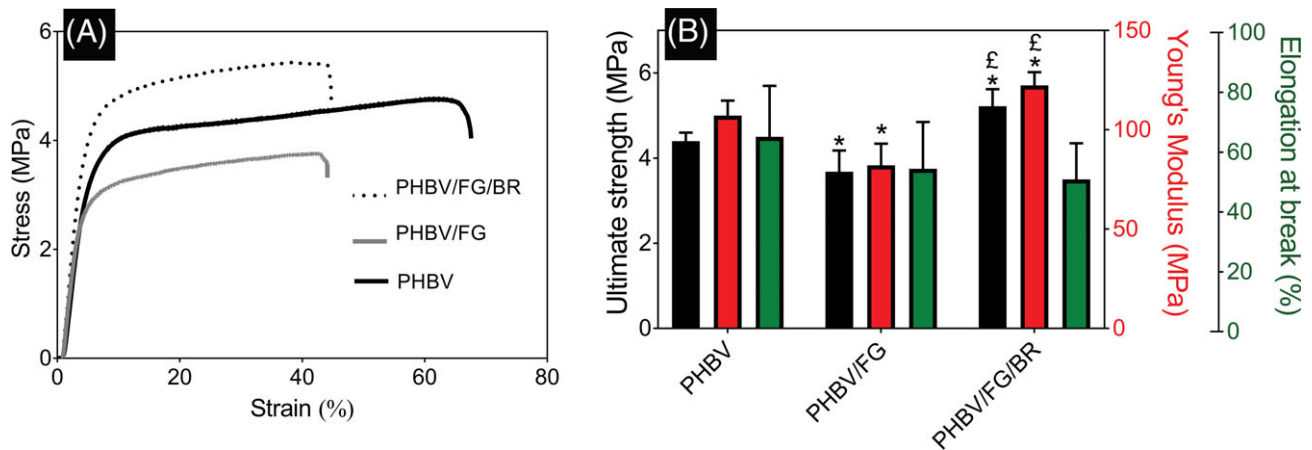


FIGURE 4. Mechanical properties of the membranes, (A) Stress–strain curves of PHBV, PHBV/FG and PHBV/FG/BR nanofibrous membranes and (B) effect of membranes compositions on the ultimate strength, Young's modulus and elongation at break of the membranes (* indicates a significant difference relative to PHBV membranes ($p \leq 0.05$), ‡ indicates a significant difference relative to PHBV/FG membranes ($p \leq 0.05$). BR, bredigite; FG, fibrinogen; PHBV, poly (hydroxybutyrate-co-3-hydroxyvalerate).

to PHBV (106.7 ± 18.2 MPa and 4.4 ± 0.5 MPa). However, the inclusion of the BR nanoparticles within the nanofibers caused a significant increase in Young's modulus and tensile strength of PHBV/FG/BR (121 ± 14.4 MPa and 5.22 ± 0.7 MPa) compared to PHBV/FG and PHBV membranes ($p \leq 0.05$).

In vitro biodegradation of the nanofibrous membranes

In vitro degradation of PHBV, PHBV/FG, and PHBV/FG/BR nanofibrous membranes were studied by monitoring the morphological changes and measuring the weight losses of the membranes during incubation in PBS at 37°C . Figure 5A–G shows the FESEM images of the nanofibrous membranes on day 14 and 28 after incubation in PBS and the weight loss of the membranes versus incubation time are plotted in Figure 5H. As shown in Figure 5, pure PHBV nanofibrous membranes showed no morphological changes after 14 and 28 days immersion in PBS and the results of weight loss measurement demonstrated only 3.2% weight loss for pure PHBV after 28 days of degradation test. PHBV/FG and PHBV/FG/BR demonstrated more morphological changes after 14 and 28 days such as fiber adhesion in some parts and the reduction in fiber diameters. Moreover, it is obvious in the high-resolution image of PHBV/FG/BR membrane (Fig. 5G) that the structure of the nanofiber changed to the porous fiber due to the production of small holes within the nanofibers as a result of fibrinogen degradation in PBS. Rapid weight loss of PHBV/FG and PHBV/FG/BR nanofibers occurred within first 4 days of degradation test (18% and 23%, respectively). The weight loss was then continued during degradation up to 28 days with a slower rate of 28% and 33%, respectively. Hence, the incorporation of fibrinogen and BR into PHBV polymer increased its ability to absorb water during immersion in PBS and, consequently, increased its hydrolytic degradation.

Cell culture

The proliferation of hFob cells on PHBV, PHBV/FG, and PHBV/FG/BR membranes after 5, 10, and 15 days of culturing

was investigated using MTS assay and the results are given in Figure 6a. The cell proliferation rate of all substrates increased during culture time, and at each time point, PHBV membranes showed the lowest proliferation rate. The proliferation of hFob incubated on PHBV/FG membranes was found to be 37% and 40.7% higher than that on PHBV membranes after 10 and 15 days, respectively, due to the presence of fibrinogen. Similarly, the MTS results revealed that PHBV/FG/BR membranes exhibited the highest proliferation of hFob among other substrates on day 10 and 15. The proliferation of hFob on PHBV/FG/BR membranes on day 15 was found to be 61.1% and 14.5% higher than PHBV and PHBV/FG membranes, respectively.

ALP activity showed increased levels in all samples from day 5 to day 15, which was in agreement with increased proliferation and maturation of hFob cells (Fig. 6B). The ALP secretion of the cells grown on PHBV/FG membranes was shown to be 26% and 29% higher than that on PHBV membranes on day 10 and 15 after cell seeding, respectively. Moreover, the PHBV/FG/BR nanofibrous membranes displayed significantly higher ALP activity than PHBV/FG membrane on day 15 ($p \leq 0.05$), due to the synergetic effect of fibrinogen and BR on the cellular activity.

ARS staining of the cells cultured on the nanofibrous membranes was performed to study the mineralization of hFob cells. The results of quantitative and qualitative analysis of ARS staining are shown in Figure 7. As it is obvious from the microscopic images, the cells on PHBV/FG/BR nanofibrous membranes induced denser bright red spots (ARS-calcium chelating products), indicating more mineral deposition than other membranes and TCP. It is clear from the plot (Fig. 7B) that after 15 days of cell culture, the eluted solution collected from PHBV/FG/BR membranes found to be 20% and 56% higher than those collected from PHBV/FG and PHBV membranes, respectively.

Cellular morphology and the mineral secretion of the cells seeded on various membranes were visualized by FESEM. Figure 8 shows the morphology and density of hFob

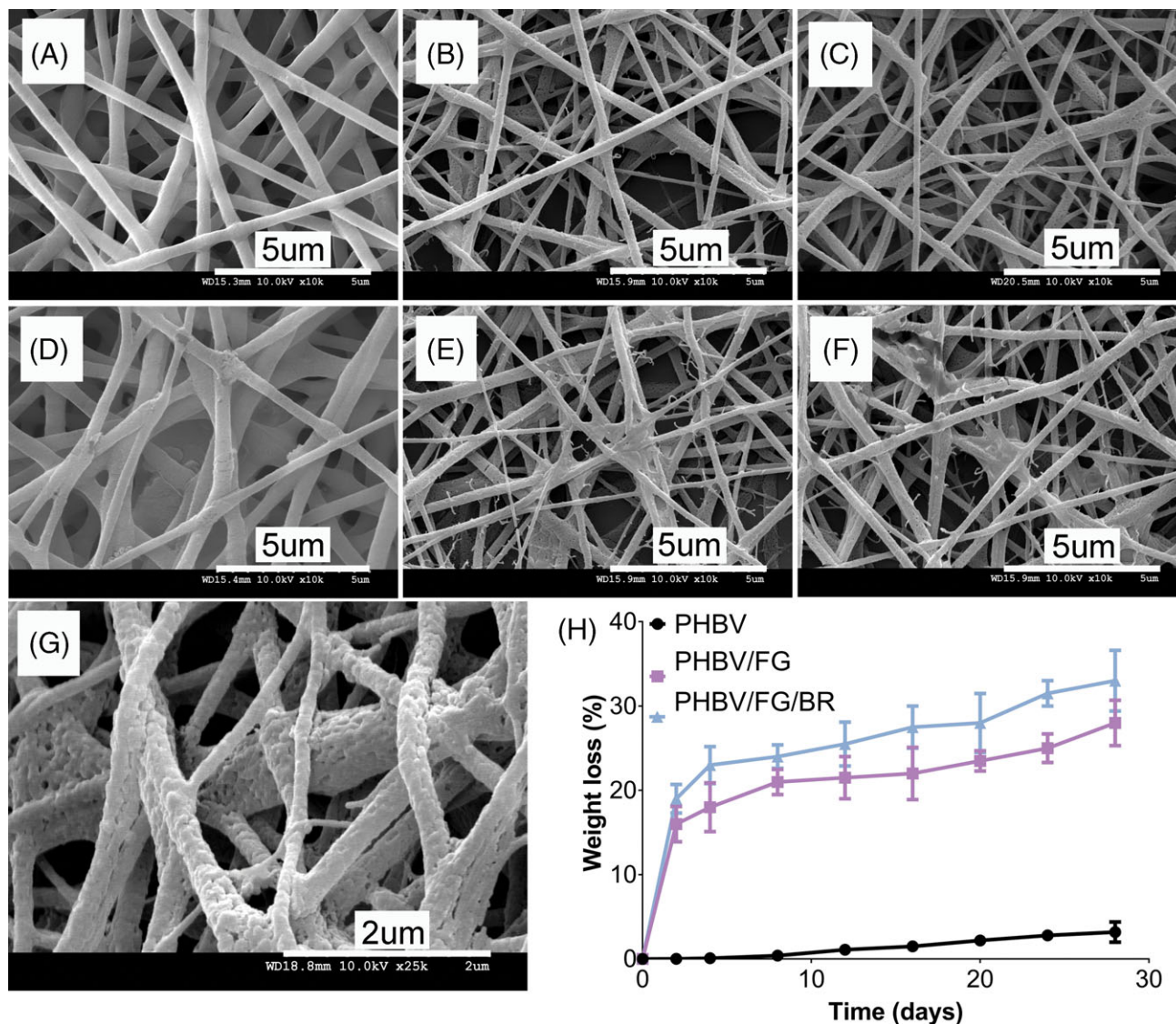


FIGURE 5. FESEM images of (A and D) PHBV, (B and E) PHBV/FG and (C, F, and G) PHBV/FG/BR nanofibrous membranes after (A–C) 2 and (D–G) 4 weeks of degradation in PBS, and (H) weight loss of PHBV, PHBV/FG, and PHBV/FG/BR membranes as function of soaking time (n = 6 samples). BR, bredigite; FESEM, field-emission scanning electron microscopy; FG, fibrinogen; PBS, phosphate-buffered saline; PHBV, poly (hydroxybutyrate-co-3-hydroxyvalerate).

cells on PHBV, PHBV/FG, and PHBV/FG/BR membranes for 5 and 15 days. After 5 days of cell seeding, the cells on PHBV/FG and PHBV/FG/BR spread more fully with the physical attachment to the neighboring cells through multiple extensions compared to PHBV membranes. Moreover, the incubated cells on PHBV/FG/BR membranes exhibited the formation of many more mineralized deposits on the surface of osteoblast cells compared to those on PHBV/FG and PHBV membranes. Higher mineral production ability of the hFob on PHBV/FG/BR membranes was confirmed by EDS analysis of the cells. Figure 9 shows the EDS patterns along with the atomic percentage of elements produced by osteoblast cells grown on the different substrates, obtained from EDS analysis on day 15. The results of EDS analysis showed that the amount of calcium and phosphorous deposits produced by cells on PHBV/FG and PHBV/FG/BR

nanofibrous membranes was higher than those on PHBV membranes. Further, the results of EDS analysis demonstrated the occurrence of the higher content of calcium and phosphorus deposition on the cultured hFob cells on PHBV/FG/BR nanofibrous membranes compared to PHBV and PHBV/FG membranes, proving its higher bone tissue forming ability.

DISCUSSION

Electrospun nanofibrous materials, mimicking the natural ECM, have been widely investigated for tissue regeneration applications. In the context of guided bone regeneration, these nanofibrous materials are utilized as membranes to have barrier function which prevent diffusion of fibroblast and epithelial cells into the defect site and enhance bone

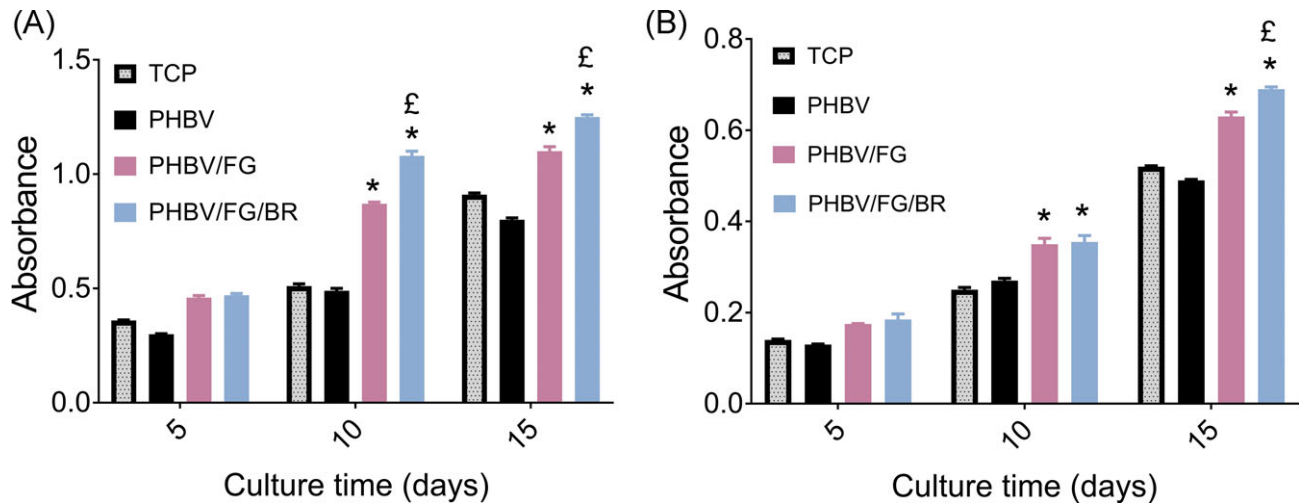


FIGURE 6. Cell proliferation and ALP activity on various membranes, (A) proliferation of hFob cells determined by MTS assay on PHBV, PHBV/FG, PHBV/FG/BR membranes, and TCP on day 5, 10, and 15, (B) ALP activity of hFob after incubation on PHBV, PHBV/FG, PHBV/FG/BR membranes, and TCP on day 5, 10, and 15, * indicates a significant difference relative to PHBV membranes ($p \leq 0.05$), £ indicates a significant difference relative to PHBV/FG membranes ($p \leq 0.05$). ALP, alkaline phosphatase; BR, bredigite; FG, fibrinogen; hFob, human fetal osteoblast; PHBV, poly (hydroxybutyrate-co-3-hydroxyvalerate); TCP, tissue culture plastic.

reconstruction by increasing osteoblast adhesion and proliferation. Among the variety of polymers investigated as nanofibrous materials for bone tissue engineering, PHBV attracted more attention due to its natural origin, suitable mechanical properties, biocompatibility and biodegradability. The combination of PHBV with bioactive biological materials is reported to be more desirable in generating nanofibrous materials for bone tissue engineering, since pure PHBV polymer naturally has some shortcoming such hydrophobic surface, lack of bioactivity and poor cellular responses. In the present study, we reported the development of PHBV nanofibrous membranes containing fibrinogen and BR with applicability in guided bone regeneration. The electrospun PHBV, PHBV/FG, and PHBV/FG/BR membranes were successfully obtained with interconnected fibrous porous structures composed of randomly oriented fibers. The beadless and relatively uniform PHBV nanofibers exhibited a fiber diameter of 410 ± 61 nm, while the blended PHBV/FG nanofibers showed lower mean fiber diameter with wider diameter distribution compared to pure PHBV nanofibers. A similar observation was reported in the literature, whereby the fiber diameter of blended fibrinogen nanofiber was found to be decreased by increasing the concentration of fibrinogen in the blended scaffolds.^{16,27} The diameter of the electrospun nanofibers is influenced by the properties of polymer solutions such as conductivity, surface tension, elasticity and viscosity. Fibrinogen is a macromolecular amphiprotic electrolyte; hence, its incorporation into the polymer solution increases the charge density and conductivity of the solution. The higher conductivity and charge density imposes higher elongation forces on the spinning solution under the electrical field, which results in the smaller fiber diameters.²⁷ The inclusion of the BR in the PHBV/FG nanofibers increased the mean fiber diameter of PHBV/FG/BR nanofibers. However, compared to pure PHBV nanofibers, PHBV/FG/BR showed the smaller fiber diameter,

which can be in favor of cell adhesion, proliferation and mineralization.²⁸

The wettability of a membrane regulates the biological functions, such as cell adhesion, spreading and proliferation by affecting the surface energy of the membrane, consequently, influencing the absorption of serum proteins on the membrane surface.²⁹ PHBV nanofibrous membranes showed the water contact angle of $129^\circ \pm 6^\circ$ due to its hydrophobic nature. The incorporation of fibrinogen enhanced the hydrophilicity of PHBV/FG membranes which can be ascribed to the available carboxyl and amine groups in the structure of fibrinogen. The PHBV/FG/BR membranes exhibited a more hydrophilic surface compared to PHBV and PHBV/FG membrane as a result of the presence of BR nanoparticles. Such hydrophilic characteristic of the PHBV/FG/BR composite membranes might lead to a better cell adhesion and proliferation. Pore size is another important property of a GBR membrane, which has a close relation to the tissue occlusivity and major effects on the soft tissue cells invasion. In addition, membrane pores can facilitate the diffusion of oxygen, fluids, nutrients, and bioactive molecules which is essential for cell and tissue growth.³⁰⁻³² In this study, the smaller fiber diameter of PHBV/FG membrane compared to PHBV membrane lead to the lower membrane pore diameter. Similarly, the PHBV/FG/BR membranes with higher fiber diameter compared to PHBV/FG showed the higher membrane pore diameter. When the diameter of the nanofibers reduced, more layers of fibers can overlap together, which results in smaller pore size.³³ Considering the application to GBR membranes, the pore size ranges obtained in this study is adequate to supply nutrients, oxygen, and fluids for cell growth on porous membranes.³⁴

Mechanical properties of a membrane are essential for understanding its performance in bone regeneration applications. The results of mechanical strength test demonstrated

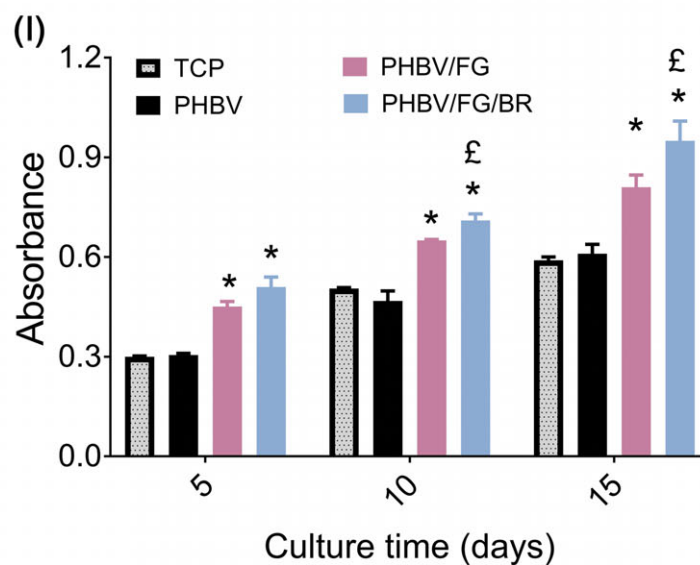
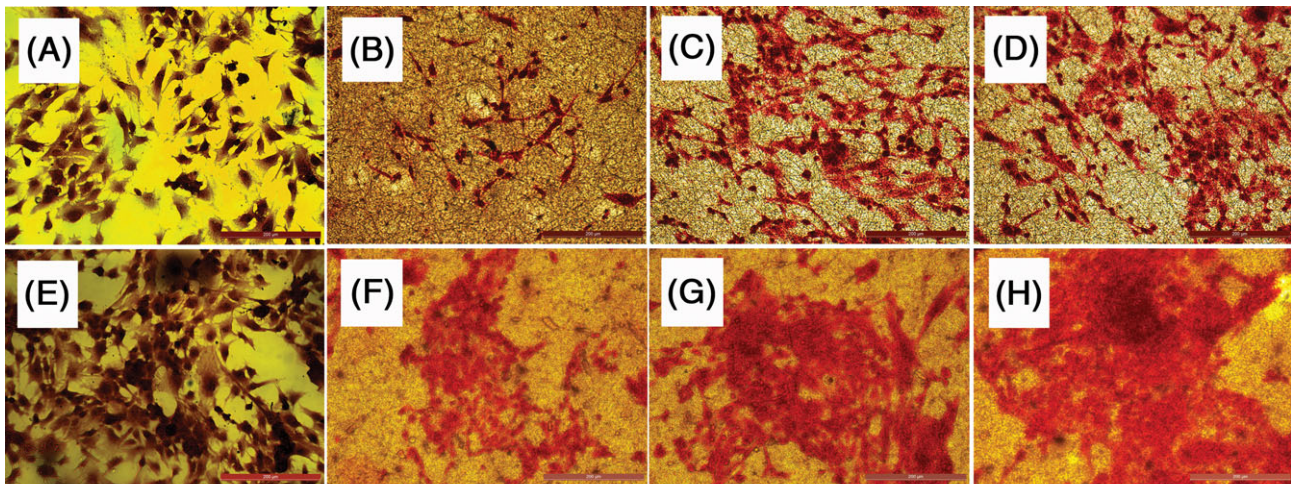


FIGURE 7. ARS staining of calcium deposition on TCP (A and E), PHBV (B and F), PHBV/FG (C and G), PHBV/FG/BR (D and H) nanofibrous membranes on day 5 (A–D) and 10 (E–H) and Quantitative estimation of calcium deposition by cetylpyridinium bromide assay on nanofibrous membranes and TCP on day 5, 10 and 15 (I), * indicates a significant difference relative to PHBV membranes ($p \leq 0.05$), £ indicates a significant difference relative to PHBV/FG membranes ($p \leq 0.05$). ARS, alizarin red-S; BR, bredigite; FG, fibrinogen; PHBV, poly (hydroxybutyrate-co-3-hydroxy-valerate); TCP, tissue culture plastic.

that Young's modulus and tensile strength of PHBV nanofibrous membranes got decreased upon blending with fibrinogen. Although fibrinogen is a highly bioactive biomaterial but shows limited mechanical integrity compared to synthetic polymers.^{16,35–37} Incorporation of BR nanoparticles within the nanofibers resulted in a significant increase in Young's modulus and tensile strength of PHBV/FG/BR compared to PHBV/FG and PHBV membranes. In our previous study, it was demonstrated that the addition of BR nanoparticles into PHBV nanofibers up to 10% resulted in improved tensile strength and increased resistance to deformation of PHBV membranes because of the reinforcement effect of BR nanoparticles within the polymer matrix.¹⁷ The increases in stiffness and strength of PHBV/FG/BR membranes can be considered as an advantageous aspect, especially for the bone tissue regeneration.

Besides the needful suitable mechanical characteristics, the biodegradation property is another important parameter determining the applicability of a GBR membrane. *in vitro* degradation performed in PBS revealed that PHBV/FG and PHBV/FG/BR nanofibrous membranes exhibited more morphological changes and higher degradation rate than pure PHBV membranes after 28 days incubation in PBS. PHBV is a hydrophobic polymer and inhibits fast diffusion of water molecules into the polymer matrix, therefore, it hardly degrades in neutral pH media without the enzymes.^{17,38,39} A common characteristic of natural biopolymers such as fibrinogen is their relatively high degradation rate in the physiological medium. On the other hand, BR is a Si-based bioceramic which hydrolyzes in the biological environment within the release of Si ions.^{14,23} Hence, the incorporation of fibrinogen and BR into PHBV matrix increases its hydrolytic

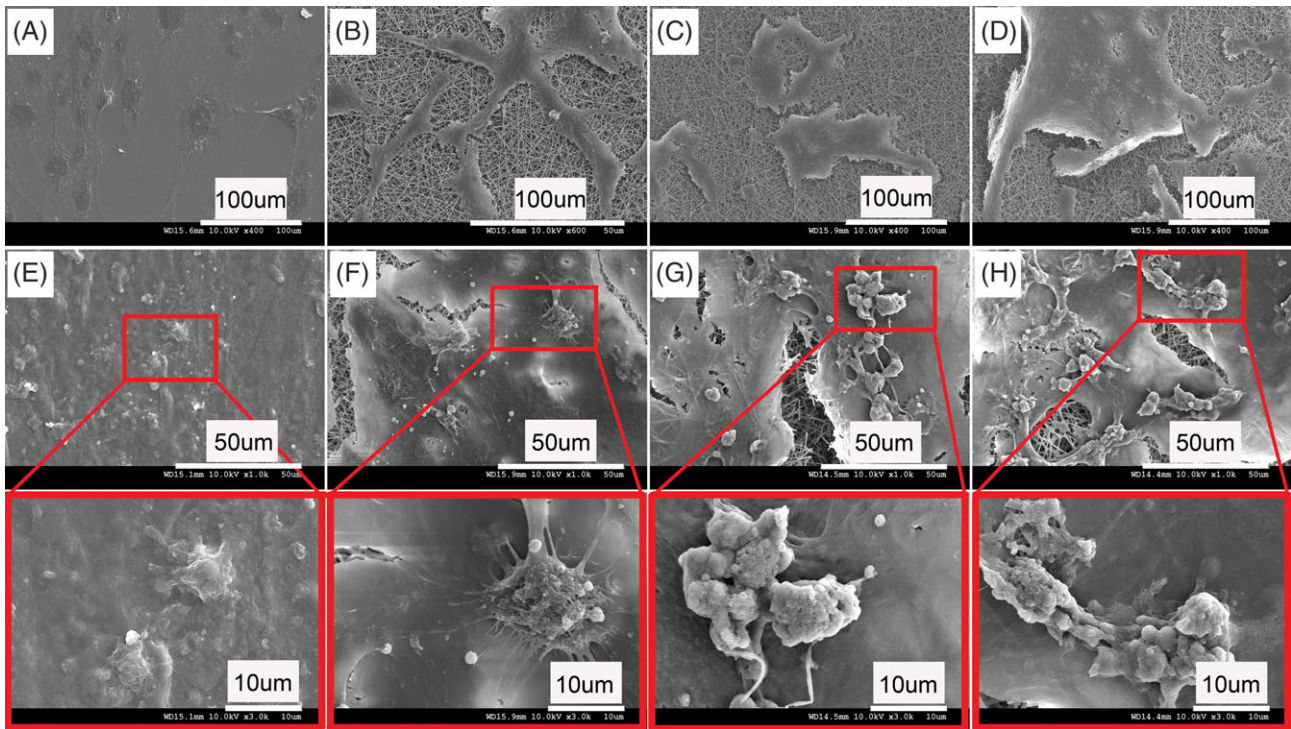


FIGURE 8. SEM micrographs showing the morphology and mineralization of hFob cells on nanofibrous membranes: TCP (A and E), PHBV (B and F), PHBV/FG (C and G), PHBV/FG/BR (D and H) nanofibrous membranes on day 5 (A–D) and 15 (E–H). BR, bredigite; FG, fibrinogen; hFob, human fetal osteoblast; PHBV, poly (hydroxybutyrate-co-3-hydroxyvalerate); SEM, scanning electron microscopy; TCP, tissue culture plastic.

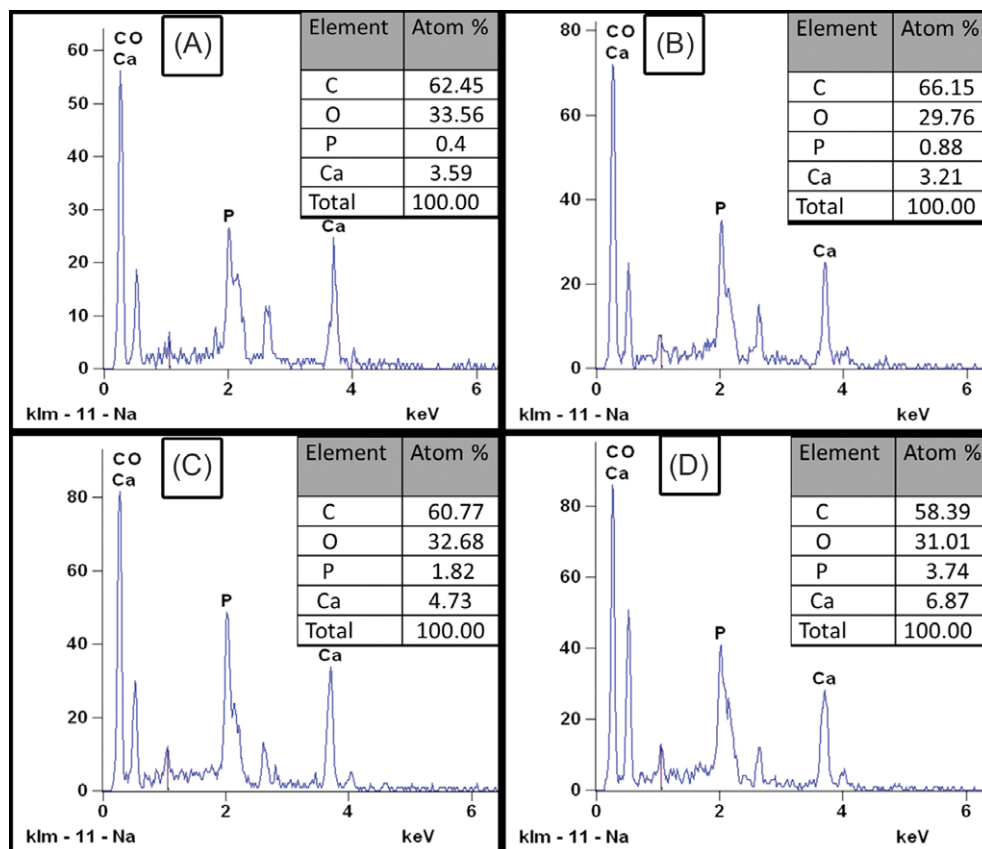


FIGURE 9. EDS analysis of the mineral deposition on (A) TCP, (B) PHBV, (C) PHBV/FG, and (D) PHBV/FG/BR after 15 days of cell culture. BR, bredigite; EDS, energy dispersive X-ray spectroscopy; FG, fibrinogen; PHBV, poly (hydroxybutyrate-co-3-hydroxyvalerate); TCP, tissue culture plastic.

degradation, making it more applicable as a resorbable membrane in guided bone regeneration.

The materials which are applied for fabricating an ideal GBR membrane must also provide an appropriate environment for cellular activity such as cell attachment, proliferation and differentiation as well as allow for tissue regeneration.⁴⁰ It is well known that surface wettability of the biomaterials is an important factor affecting osteoblast adhesion and proliferation. So, the hydrophobic surface of PHBV membranes (according to the water contact angle measurement) is the reason for its lowest cell attachment and proliferation, when compared to other samples. The higher proliferation rate of hFob on the PHBV/FG membranes compared to PHBV membranes is attributed to the presence of fibrinogen. Fibrinogen is a fibrous glycoprotein which is essential for many biological processes and has the inherent ability to induce cellular activity. Numerous studies have confirmed the positive impact of applying fibrinogen on the *in vitro* cell adhesion, proliferation, and differentiation as well as *in vivo* bone healing/remodeling in bone regeneration applications.^{41–44} The MTS assay results also revealed that hFob cells proliferated better on PHBV/FG/BR membranes compared to PHBV/FG, due to the BR nanoparticles inclusion. Studies have demonstrated that Mg and Si containing bioceramics can enhance cell adhesion, spreading, proliferation, and differentiation into the osteoblasts.^{45,46}

ALP activity is a marker of the early stage of cell differentiation, since its level increases with the osteoblast cells maturation. The secretion of ALP regulates the structure of ECM to progress to the mineralization stage.⁴⁷ By increasing the cell proliferation, ALP secretion got increased on all nanofibrous membranes, however, the ALP activity of the cells increased more on the PHBV/FG/BR membranes than on the PHBV and PHBV/FG membranes. The higher level of ALP activity observed on the PHBV/FG/BR membranes indicates the higher osteoblast activity of hFob, highlighting a significant synergetic effect between fibrinogen and BR on hFob differentiation and mineralization.

In the context of guided bone tissue regeneration, nanofibrous membranes should not only promote cell attachment, proliferation, and differentiation but also induce mineral formation in the physiological media, which would, in turn, accelerate bone formation. The cultured cells on PHBV/FG/BR and PHBV/FG membranes induced more mineral deposition compared to PHBV membrane as shown by ARS results, moreover, mineralization level of hFob cells on PHBV/FG/BR was found to be higher than on PHBV/FG membranes, which can be due to the contributory effect of fibrinogen and BR, confirming the osteogenic potential of cells seeded on PHBV/FG/BR membranes over the other membranes.

Morphological evidence revealed an increase in cell density with incubation time for all nanofibrous membranes with the formation of multilayered mineral particles on the surface of the cells, indicating the confluent cell growth and cell-secreted mineralization. Further, PHBV/FG/BR nanofibrous membranes induced many more mineralized materials formation on the surface of the cells, suggesting that fibrinogen and BR are in favor of calcification of the

hFob cells, which was then confirmed by the obtained results from EDS analysis. The results of EDS analysis again confirmed the higher mineralization and bone formation ability of PHBV/FG/BR nanofibrous membrane compared to PHBV and PHBV/FG membranes. Overall, the results showed that PHBV/FG/BR nanofibrous membranes developed in this study have great potential of using as membranes for guided bone tissue engineering applications.

CONCLUSION

Electrospun PHBV/FG/BR nanofibrous membranes were fabricated and their biological properties were evaluated toward guided bone tissue engineering applications. The obtained results demonstrated that the mean fiber diameter and membrane pore size decreased with the addition of fibrinogen and further increased by incorporation of BR nanoparticles. The mechanical and thermal properties of resultant membranes were found to be affected by nanofibers compositions. The hydrophilicity and degradation rate of PHBV membranes increased upon the incorporation of fibrinogen and BR, which were in favor of cell response for proliferation and mineralization. *in vitro* biological evaluation revealed that the osteoblast cells cultured on PHBV/FG/BR nanofibrous membranes exhibited higher cell proliferation and increased ALP activity and calcium mineral deposition up to 15 days of cell culture when compared to PHBV and PHBV/FG membranes. The experimental data demonstrated that the developed electrospun PHBV/FG/BR nanofibrous membranes have great potential to be used for guided bone tissue engineering applications.

REFERENCES

1. Park JK, Yeom J, Oh EJ, Reddy M, Kim JY, Cho D-W, Lim HP, Kim NS, Park SW, Shin H-I. Guided bone regeneration by poly(lactic-co-glycolic acid) grafted hyaluronic acid bi-layer films for periodontal barrier applications. *Acta Biomater* 2009;5(9):3394–3403.
2. Xue J, He M, Liu H, Niu Y, Crawford A, Coates PD, Chen D, Shi R, Zhang L. Drug loaded homogeneous electrospun PCL/gelatin hybrid nanofiber structures for anti-infective tissue regeneration membranes. *Biomaterials* 2014;35(34):9395–9405.
3. Gentile P, Chiono V, Tonda-Turo C, Ferreira AM, Ciardelli G. Polymeric membranes for guided bone regeneration. *Biotechnol J* 2011; 6(10):1187–1197.
4. Lee EJ, Shin DS, Kim HE, Kim HW, Koh YH, Jang JH. Membrane of hybrid chitosan-silica xerogel for guided bone regeneration. *Biomaterials* 2009;30(5):743–750.
5. Zhang S, Huang Y, Yang X, Mei F, Ma Q, Chen G, Ryu S, Deng X. Gelatin nanofibrous membrane fabricated by electrospinning of aqueous gelatin solution for guided tissue regeneration. *J Biomed Mater Res A* 2009;90A(3):671–679.
6. Qasim SB, Delaine-Smith RM, Fey T, Rawlinson A, Rehman IU. Freeze gelled porous membranes for periodontal tissue regeneration. *Acta Biomater* 2015;23:317–328.
7. Fu S, Ni P, Wang B, Chu B, Peng J, Zheng L, Zhao X, Luo F, Wei Y, Qian Z. *In vivo* biocompatibility and osteogenesis of electrospun poly(epsilon-caprolactone)-poly(ethylene glycol)-poly(epsilon-caprolactone)/nano-hydroxyapatite composite scaffold. *Biomaterials* 2012; 33(33):8363–8371.
8. Cool SM, Kenny B, Wu A, Nurcombe V, Trau M, Cassady AI, Grøndahl L. Poly(3-hydroxybutyrate-co-3-hydroxyvalerate) composite biomaterials for bone tissue regeneration: *in vitro* performance assessed by osteoblast proliferation, osteoclast adhesion and resorption, and macrophage proinflammatory response. *J Biomed Mater Res A* 2007;82A(3):599–610.
9. Ke Y, Wang YJ, Ren L, Zhao QC, Huang W. Modified PHBV scaffolds by *in situ* UV polymerization: Structural characteristic,

- mechanical properties and bone mesenchymal stem cell compatibility. *Acta Biomater* 2010;6(4):1329–1336.
10. Nobes GAR, Maysinger D, Marchessault RH. Polyhydroxyalkanoates: Materials for delivery systems. *Drug Deliv* 1998;5(3):167–177.
 11. Wang A, Gan Y, Yu H, Liu Y, Zhang M, Cheng B, Wang F, Wang H, Yan J. Improvement of the cytocompatibility of electrospun poly [(R)-3-hydroxybutyrate-co-(R)-3-hydroxyvalerate] mats by Ecoflex. *J Biomed Mater Res A* 2012;100A(6):1505–1511.
 12. Wu C, Chang J. Synthesis and in vitro bioactivity of bredigite powders. *J Biomater Appl* 2007;21(3):251–263.
 13. Wu C, Chang J, Wang J, Ni S, Zhai W. Preparation and characteristics of a calcium magnesium silicate (bredigite) bioactive ceramic. *Biomaterials* 2005;26(16):2925–2931.
 14. Zhou Y, Wu C, Zhang X, Han P, Xiao Y. The ionic products from bredigite bioceramics induced cementogenic differentiation of periodontal ligament cells via activation of the Wnt/ β -catenin signalling pathway. *J Mater Chem B* 2013;1(27):3380.
 15. Wang J, Wang H, Wang Y, Li J, Su Z, Wei G. Alternate layer-by-layer assembly of graphene oxide nanosheets and fibrinogen nanofibers on a silicon substrate for a biomimetic three-dimensional hydroxyapatite scaffold. *J Mater Chem B* 2014;2(42):7360–7368.
 16. He C, Xu X, Zhang F, Cao L, Feng W, Wang H, Mo X. Fabrication of fibrinogen/P(LLA-CL) hybrid nanofibrous scaffold for potential soft tissue engineering applications. *J Biomed Mater Res A* 2011;97(3):339–347.
 17. Kouhi M, Prabhakaran MP, Shamanian M, Fathi M, Morshed M, Ramakrishna S. Electrospun PHBV nanofibers containing HA and bredigite nanoparticles: Fabrication, characterization and evaluation of mechanical properties and bioactivity. *Compos Sci Technol* 2015;121:115–122.
 18. Murugan R, Ramakrishna S. Development of nanocomposites for bone grafting. *Compos Sci Technol* 2005;65(15):2385–2406.
 19. Kouhi M, Fathi M, Prabhakaran MP, Shamanian M, Ramakrishna S. Poly L lysine-modified PHBV based nanofibrous scaffolds for bone cell mineralization and osteogenic differentiation. *Appl Surf Sci* 2018;457:616–625.
 20. Jayaraman K, Kotaki M, Zhang Y, Mo X, Ramakrishna S. Recent advances in polymer nanofibers. *J Nanosci Nanotechnol* 2004;4(1–1):52–65.
 21. Holzwarth JM, Ma PX. Biomimetic nanofibrous scaffolds for bone tissue engineering. *Biomaterials* 2011;32(36):9622–9629.
 22. Yang F, Both SK, Yang X, Walboomers XF, Jansen JA. Development of an electrospun nano-apatite/PCL composite membrane for GTR/GBR application. *Acta Biomater* 2009;5(9):3295–3304.
 23. Kouhi M, Shamanian M, Fathi M, Samadikuchaksaraei A, Mehdipour A. Synthesis, characterization, in vitro bioactivity and biocompatibility evaluation of hydroxyapatite/Bredigite (Ca₇MgSi₄O₁₆) composite nanoparticles. *JOM* 2016;68(4):1061–1070.
 24. Jack KS, Velayudhan S, Luckman P, Trau M, Grøndahl L, Cooper-White J. The fabrication and characterization of biodegradable HA/PHBV nanoparticle–polymer composite scaffolds. *Acta Biomater* 2009;5(7):2657–2667.
 25. Boix M, Eslava S, Costa Machado G, Gosselin E, Ni N, Saiz E, De Coninck J. ATR-FTIR measurements of albumin and fibrinogen adsorption: Inert versus calcium phosphate ceramics. *J Biomed Mater Res A* 2015;103(11):3493–3502.
 26. Kouhi M, Jayarama Reddy V, Ramakrishna S. GPTMS-modified Bredigite/PHBV Nanofibrous bone scaffolds with enhanced mechanical and biological properties. *Appl Biochem Biotechnol* 2018;186:1–12. <https://doi.org/10.1007/s12010>.
 27. Fang Z, Fu W, Dong Z, Zhang X, Gao B, Guo D, He H, Wang Y. Preparation and biocompatibility of electrospun poly(l-lactide-co- ϵ -caprolactone)/fibrinogen blended nanofibrous scaffolds. *Appl Surf Sci* 2011;257(9):4133–4138.
 28. Chen M, Patra PK, Warner SB, Bhowmick S. Role of fiber diameter in adhesion and proliferation of NIH 3T3 fibroblast on electrospun polycaprolactone scaffolds. *Tissue Eng* 2007;13(3):579–587.
 29. Bacakova L, Filova E, Parizek M, Ruml T, Svorcik V. Modulation of cell adhesion, proliferation and differentiation on materials designed for body implants. *Biotechnol Adv* 2011;29(6):739–767.
 30. Elgali I, Omar O, Dahlin C, Thomsen P. Guided bone regeneration: Materials and biological mechanisms revisited. *Eur J Oral Sci* 2017;125(5):315–337.
 31. Oh SH, Kim JH, Kim JM, Lee JH. Asymmetrically porous PLGA/Pluronic F127 membrane for effective guided bone regeneration. *J Biomater Sci Polym Ed* 2006;17(12):1375–1387.
 32. Gutta R, Baker RA, Bartolucci AA, Louis PJ. Barrier membranes used for ridge augmentation: Is there an optimal pore size? *J Oral Maxillofac Surg* 2009;67(6):1218–1225.
 33. Ghasemi-Mobarakeh L, Prabhakaran MP, Morshed M, Nasr-Esfahani MH, Ramakrishna S. Bio-functionalized PCL nanofibrous scaffolds for nerve tissue engineering. *Mater Sci Eng C* 2010;30(8):1129–1136.
 34. Maeda H, Kasuga T, Hench LL. Preparation of poly(L-lactic acid)-polysiloxane-calcium carbonate hybrid membranes for guided bone regeneration. *Biomaterials* 2006;27(8):1216–1222.
 35. Francis MP, Moghaddam-White YM, Sachs PC, Beckman MJ, Chen SM, Bowlin GL, Elmore LW, Holt SE. Modeling early stage bone regeneration with biomimetic electrospun fibrinogen nanofibers and adipose-derived mesenchymal stem cells. *Electrospinning* 2016;1(1):10–19.
 36. McManus MC, Boland ED, Koo HP, Barnes CP, Pawlowski KJ, Wnek GE, Simpson DG, Bowlin GL. Mechanical properties of electrospun fibrinogen structures. *Acta Biomater* 2006;2(1):19–28.
 37. Sell SA, Francis MP, Garg K, McClure MJ, Simpson DG, Bowlin GL. Cross-linking methods of electrospun fibrinogen scaffolds for tissue engineering applications. *Biomed Mater* 2008;3(4):045001.
 38. Li H, Chang J. In vitro degradation of porous degradable and bioactive PHBV/wollastonite composite scaffolds. *Polym Degrad Stab* 2005;87(2):301–307.
 39. Majid MIA, Ismail J, Few LL, Tan CF. The degradation kinetics of poly(3-hydroxybutyrate) under non-aqueous and aqueous conditions. *Eur Polym J* 2002;38(4):837–839.
 40. Rajangam T, An SS. Fibrinogen and fibrin based micro and nano scaffolds incorporated with drugs, proteins, cells and genes for therapeutic biomedical applications. *Int J Nanomed* 2013;8:3641–3662.
 41. Khadka DB, Haynie DT. Protein- and peptide-based electrospun nanofibers in medical biomaterials. *Nanomedicine* 2012;8(8):1242–1262.
 42. Noori A, Ashrafi SJ, Vaez-Ghaemi R, Hatamian-Zaremi A, Webster TJ. A review of fibrin and fibrin composites for bone tissue engineering. *Int J Nanomed* 2017;12:4937–4961.
 43. Kim BS, Lee J. Enhanced bone healing by improved fibrin-clot formation via fibrinogen adsorption on biphasic calcium phosphate granules. *Clin Oral Implants Res* 2015;26(10):1203–1210.
 44. Santos SG, Lamghari M, Almeida CR, Oliveira MI, Neves N, Ribeiro AC, Barbosa JN, Barros R, Maciel J, Martins MCL. Adsorbed fibrinogen leads to improved bone regeneration and correlates with differences in the systemic immune response. *Acta Biomater* 2013;9(7):7209–7217.
 45. Varanasi VG, Saiz E, Loomer PM, Ancheta B, Uritani N, Ho SP, Tomsia AP, Marshall SJ, Marshall GW. Enhanced osteocalcin expression by osteoblast-like cells (MC3T3-E1) exposed to bioactive coating glass (SiO₂-CaO-P₂O₅-MgO-K₂O-Na₂O system) ions. *Acta Biomater* 2009;5(9):3536–3547.
 46. Lu W, Ji K, Kirkham J, Yan Y, Boccaccini AR, Kellett M, Jin Y, Yang XB. Bone tissue engineering by using a combination of polymer/bioglass composites with human adipose-derived stem cells. *Cell Tissue Res* 2014;356(1):97–107.
 47. Golub EE, Boesze-Battaglia K. The role of alkaline phosphatase in mineralization. *Curr Opin Orthopaed* 2007;18(5):444–448.